

## Magnetotransport in perovskite series $\text{La}_{n-nx}\text{Ca}_{1+nx}\text{Mn}_n\text{O}_{3n+1}$ ferromagnets

H. Asano, J. Hayakawa, and M. Matsui

Department of Crystalline Materials Science, Nagoya University, Furo-cho, Chikusa-ku, Nagoya 464-01, Japan

(Received 30 July 1997; revised manuscript received 6 October 1997)

The perovskite series  $\text{La}_{n-nx}\text{Ca}_{1+nx}\text{Mn}_n\text{O}_{3n+1}$  ( $n=2, 3$ , and  $\infty$ ) composed of  $n$  layers of  $\text{MnO}_2$  is a colossal magnetoresistance (CMR) ferromagnet. Results on the transport properties of epitaxial  $a$ -axis thin-film samples with a fixed carrier concentration ( $x=0.3$ ) have indicated that a reduction in the number of layers results in systematic changes in the various features. These include an increase in resistivity, a decrease in the resistivity peak temperature  $T_c^p$  corresponding to the metal-insulator transition, an enhancement of the maximum MR near  $T_c^p$ , and an increase in the low-temperature intrinsic MR. In order to explain the variation in these features with the number of  $\text{MnO}_2$  layers, it is necessary to take both  $c$ -axis transfer interaction and two-dimensional spin fluctuation into account. [S0163-1829(98)03302-5]

The observation of the colossal magnetoresistance (CMR) effect<sup>1-6</sup> in the mixed valence manganese perovskites has revived interest in the physical (magnetic and electrical) properties of this class of compounds. The ferromagnetic metallic state in these compounds has been explained by the double exchange theory, which considers the transfer of an electron between  $\text{Mn}^{3+}$ -O- $\text{Mn}^{4+}$  ions.<sup>7-9</sup> As a result of strong Hund exchange coupling, the itinerant  $e_g^1$  electrons (holes) interact with the localized  $t_{2g}^3$  electrons ( $S = \frac{3}{2}$ ), and thus mediate ferromagnetic ordering. Several studies on the pseudocubic perovskites  $\text{La}_{1-x}\text{M}_x\text{MnO}_3$  ( $M = \text{Ca}, \text{Sr}$ ) have shown that materials with an optimized carrier concentration  $x \sim 0.3$ , which undergo a transition from the paramagnetic insulator state to the ferromagnetic metal state upon cooling, exhibit CMR in a narrow temperature range around the Curie temperature. There is strong evidence that distortion of the Mn-O-Mn bond, which modifies the one-electron bandwidth, is a crucial parameter governing spin-charge coupling, hence the magnitude of the CMR. Moreover, theoretical and experimental studies<sup>10-12</sup> have pointed out the importance of electron-phonon interaction that relates to Jahn-Teller-type lattice distortions of the  $\text{MnO}_6$  octahedra. The above results suggest that there is considerable coupling among the charge, spin, and lattice in this system.

Recent attention in this field has focused on layered perovskite series of Ruddlesden-Popper compounds  $(\text{La}-M)_{n+1}\text{Mn}_n\text{O}_{3n+1}$ , since CMR was observed in the  $n=2$  compounds ( $M = \text{Sr}, \text{Ca}$ ).<sup>13,14</sup> In contrast to pseudocubic perovskites ( $n=\infty$ ) with three-dimensional Mn-O networks, the layered versions of  $(\text{La}-M)_{n+1}\text{Mn}_n\text{O}_{3n+1}$ , of which layer sequences are shown schematically in Fig. 1, consisting of perovskite blocks,  $n$   $\text{MnO}_6$  octahedra thick, offset along the  $c$  axis and with an intervening layer of  $(\text{La}-M)\text{O}$  ions, possess a two-dimensional and anisotropic character whose magnitude depends on the  $n$  value. Apart from the  $n=1$  member, which is an antiferromagnet at any doping concentration, the layered manganites with  $n=2, 3$  and  $x \sim 0.3-0.4$  are found to be ferromagnets exhibiting CMR effects. Studies<sup>13-17</sup> of the  $n=2$  compound have shown that they exhibit remarkable features including MR ratio enhancement, anisotropy in charge transport, magnetization,

and magnetostriction, existence of two-dimensional ferromagnetic ordering at a certain temperature range, and the characteristic low-temperature intrinsic MR effect. Very recently, it has been reported that the  $n=3$  compound<sup>18</sup> exhibits some features that are similar to those observed for the  $n=2$  compound. However, the microscopic origin of several features remains unclear, and a unified interpretation explaining the variation in the features with the number of  $\text{MnO}_2$  layers in the perovskite family is not yet available.

In this paper, we present a series of results on the transport properties of  $\text{La}_{n-nx}\text{Ca}_{1+nx}\text{Mn}_n\text{O}_{3n+1}$  thin films for  $n=2, 3$ , and  $\infty$  together with a discussion of the variation in various features with different numbers of  $\text{MnO}_2$  layers. The features of present concern include electrical resistivity, metal-insulator transition  $T_c^p$ , maximum MR near  $T_c^p$ , and low-temperature tunneling MR. Based on a comparison of the magnitude of these features among the compounds, we argue that the reduced  $c$ -axis transfer interaction as well as the two-dimensional spin fluctuation, which result from the anisotropic (double) exchange interaction, play an important role in enhanced CMR and other related properties.

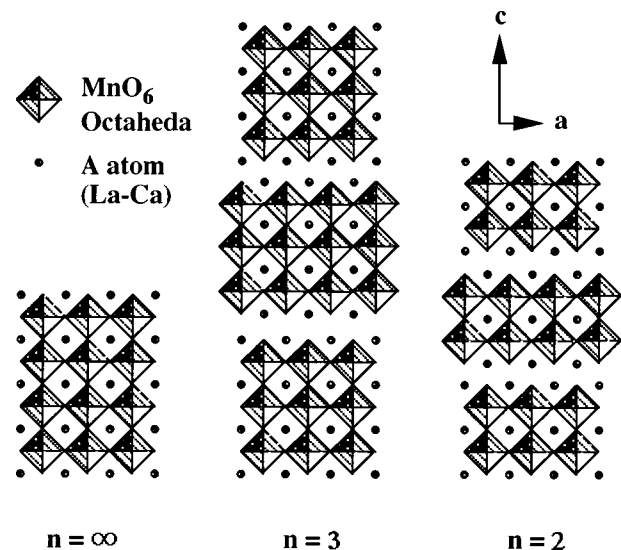


FIG. 1. Schematic views of layer sequences of  $(\text{La}-\text{Ca})_{n+1}\text{Mn}_n\text{O}_{3n+1}$  compounds.

A single-target magnetron sputtering technique was used for preparing the thin-film samples of  $\text{La}_{n-nx}\text{Ca}_{1+nx}\text{Mn}_n\text{O}_{3n+1}$  ( $n=2, 3$ , and  $\infty$ ). The preparation methods and conditions have been reported elsewhere.<sup>15</sup> The targets for the thin films of  $n=2, 3$ , and  $\infty$  compounds were disks with nominal compositions of  $\text{La}_{1.4}\text{Ca}_{1.6}\text{Mn}_2\text{O}_y$ ,  $\text{La}_{2.1}\text{Ca}_{1.9}\text{Mn}_3\text{O}_y$ , and  $\text{La}_{0.7}\text{Ca}_{0.3}\text{MnO}_y$ , respectively. The film thickness was typically 150 nm, and the substrates were MgO (001). Energy dispersive x-ray microanalysis (EDX) indicated that the compositions of the films were nearly identical to the nominal one within the accuracy ( $\sim 2\%$ ) of EDX. X-ray-diffraction analysis showed that all the films were single phase and had an  $a$ -axis (100) normal orientation to the substrate surface. The  $\phi$ -scan (in-plane rotation) x-ray analysis on the  $n=2,3$  thin films indicated that the  $a$ -axis films were ordered in the film plane and consisted of two domains, rotated at  $90^\circ$  to each other, in the plane (the so-called mosaic structure). The diffraction data including the  $\phi$ -scan mode gave us lattice parameters of  $a_0=0.3864$  nm for the  $n=\infty$  films,  $a_0=0.3864$  nm,  $c_0=1.920$  nm, and  $c_0/a_0=4.970$  for the  $n=2$  films, and  $a_0=0.3867$  nm,  $c_0=2.680$  nm, and  $c_0/a_0=6.930$  for the  $n=3$  films. The three types of samples exhibited full widths at half maximum in the rocking curve for the (200) reflection in the  $0.3\text{--}0.5^\circ$  range, indicating similar epitaxial quality.

The top panel in Fig. 2 shows the temperature dependence of the resistivity  $\rho$  in a zero field for thin-film samples of  $\text{La}_{n-nx}\text{Ca}_{1+nx}\text{Mn}_n\text{O}_{3n+1}$  with  $n=2, 3$ , and  $\infty$ . All three samples display a maximum in the  $\rho$ - $T$  curve at a respective temperature and exhibits a metallic behavior below and a semiconducting behavior above the temperature. This resistivity maximum is indicative of the occurrence of a metal-insulator (MI) transition. The MI transition temperatures  $T_c^p$ , defined by the temperature of the resistivity maximum are listed in Table I, together with other data including the resistivity values at 4.2 K and  $T_c^p$ . When comparing these thin-film data ( $n=2, \infty$ ) with those of polycrystalline bulk samples with identical  $n$  and carrier concentration values (no available data for  $n=3$  bulk sample), the present thin films exhibit  $T_c^p$  values, which are in good agreement with the bulk values [140 K (Ref. 14) for  $n=2$ , and 240 K (Ref. 4) for  $n=\infty$ ]. The slight reduction ( $\sim 10$  K) in the  $T_c^p$  values in the thin films might be due to strain induced by the substrate or slight deviation of the carrier concentrations. The thin films exhibited reasonably low-resistivity values at 4.2 K (about two orders of magnitude lower than those of the bulk samples), indicating a film epitaxial quality free from granularity.

The middle panel in Fig. 2 shows the temperature dependence of the magnetization  $M$  in a magnetic field of 1 T for thin-film samples of  $\text{La}_{n-nx}\text{Ca}_{1+nx}\text{Mn}_n\text{O}_{3n+1}$  with  $n=2, 3$ , and  $\infty$ . The ferromagnetic Curie temperatures  $T_c^M$  are determined by the conventional  $M^2$ - $T$  method. All the thin film samples possessed the  $T_c^M$  values that are correlated well with the  $T_c^p$  values. However, the three samples exhibit different behavior in the  $M$ - $T$  curves, especially at temperatures higher than the  $T_c^M$ . The inverse susceptibility  $1/\chi$ - $T$  curves at the high temperatures for the three samples are shown in the bottom panel in Fig. 2. A linear temperature dependence of  $1/\chi$  is observed above  $\sim 260$  K, and the temperatures  $\Theta_p$ ,

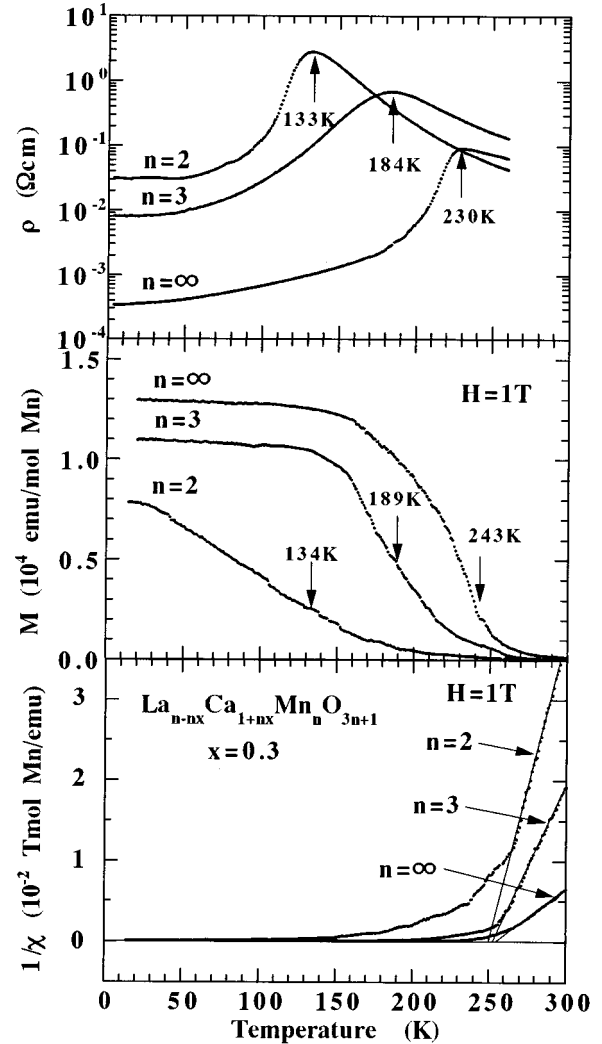


FIG. 2. Temperature dependence of resistivity  $\rho$ , magnetization  $M$ , and inverse susceptibility  $1/\chi$  for thin films of  $\text{La}_{n-nx}\text{Ca}_{1+nx}\text{Mn}_n\text{O}_{3n+1}$  with  $n=2, 3$ , and  $\infty$ . The magnetization and inverse susceptibility  $1/\chi$  are measured under an applied magnetic field of 1 T. Arrows in the top panel indicate the resistivity peak temperatures  $T_c^p$ , and arrows in the middle panel indicate the magnetic transition temperatures  $T_c^M$ .

extrapolated from the Curie-Weiss plot, are about 250 K for all the samples. Although the  $\Theta_p$  value is close to the  $T_c^M$  value for the  $n=\infty$ , the  $\Theta_p$  value is much higher than the  $T_c^M$  values for the layered compounds with  $n=2$  and 3. The large deviation between the  $T_c^M$  and the  $\Theta_p$  values has been reported for single crystals<sup>13</sup> and thin films<sup>15</sup> of the layered ( $n=2$ ) compounds. This could be interpreted as being the result of the anisotropic electron transfer and exchange interaction, which is due to the different Mn-O bond configurations in the  $a$ -axis and  $c$ -axis directions. Therefore, the upper transition temperature  $\Theta_p$  can be ascribed to the stronger  $a$ -axis interaction, and the lower one,  $T_c^M$ , to the weaker  $c$ -axis interaction.

The data listed in Table I indicate that the transport and magnetic properties are sensitively dependent on the number of  $\text{MnO}_2$  layers,  $n$ . As the  $n$  values decrease, the  $T_c^p$  and the  $T_c^M$  values decrease and the resistivity values increase dramatically. This systematic dependence on  $n$  is also observed

TABLE I. Typical physical properties of thin films of  $\text{La}_{n-nx}\text{Ca}_{1+nx}\text{Mn}_n\text{O}_{3n+1}$  with  $x=0.3$ .

$n$	$\rho$ at 4.2 K ( $\Omega$ cm)	$\rho$ at $T_c^p$ ( $\Omega$ cm)	$T_c^p$ (K)	$T_c^M$ (K)	$\Theta_p$ (K)	$(\rho(1\text{ T}) - \rho(0))/\rho(0)$ at $\sim T_c^p$ (%)	$(\rho(1\text{ T}) - \rho(0))/\rho(0)$ at 4.2 K (%)
2	$3.1 \times 10^{-2}$	$2.8 \times 10^0$	133	134	250	-93	-50
3	$8.2 \times 10^{-3}$	$6.8 \times 10^{-1}$	184	189	254	-61	-16
$\infty$	$3.4 \times 10^{-4}$	$9.2 \times 10^{-2}$	230	243	255	-50	0

for the MR behavior. The temperature dependence of the negative MR ratio  $-\Delta\rho/\rho(0)$  ( $H=1\text{ T}$ ) for the three samples is shown in Fig. 3. The MR ratio is defined as  $\Delta\rho/\rho(0)=[\rho(H)-\rho(0)]/\rho(0)$ , where  $\rho(H)$  and  $\rho(0)$  are the resistivity in an applied magnetic field and the zero-field resistivity, respectively. It is clear that all the samples exhibited maximum magnetoresistance near  $T_c^p$ . For the  $n=\infty$  compound, the relatively large MR associated with  $T_c^p$  is restricted to a narrow temperature range, and the MR ratio decreases with decreasing temperature and becomes negligible in the low-temperature range. By contrast, for the layered compound with  $n=2,3$ , we can see a broad maximum in the MR- $T$  curve and observe an appreciable MR effect over a wide temperature range from low temperature to around  $T_c^p$ . The maximum and low-temperature (4.2 K) MR values for the samples are listed in the last two lines in Table I, showing that a reduction in  $n$  resulted in remarkable enhancement of both the maximum and low-temperature MR.

We now turn to the origin of the relationship between the number of  $\text{MnO}_2$  layers,  $n$  and the electrical transport in  $\text{La}_{n-nx}\text{Ca}_{1+nx}\text{Mn}_n\text{O}_{3n+1}$ . As a consequence of the structural change from perovskite ( $n=\infty$ ) down to  $n=2$ , which is brought about by insertion of the insulating  $(\text{La,Ca})_2\text{O}_2$  layer into the perovskite layers, a two-dimensional character is introduced. This is expected to produce an anisotropic reduction of the one-electron ( $e_g$ ) bandwidth. The  $e_g$  bandwidth, as several experimental studies<sup>5,19</sup> have revealed, is the critical parameter governing the CMR and related properties in perovskite manganites. Theoretically, it is predicted that the  $e_g$  bandwidth determines the transfer interaction  $t$  between neighboring Mn sites. Within the framework of a simple double exchange theory, the exchange interaction is proportionally related to the transfer interaction  $t$ , and the ferro-

magnetic transition is associated with the MI transition. Therefore, the MI and ferromagnetic transition temperature is expected to be proportional to the effective  $e_g$  bandwidth ( $W$ ). From the transition temperature values in Table I, we can estimate the one-electron bandwidth of the  $e_g$  electrons for the three compounds. Assuming that  $W$  is 1.5 eV for  $\text{La}_{0.7}\text{Sr}_{0.3}\text{MnO}_3$  ( $T_c=360\text{ K}$ ),<sup>20</sup> the  $W$  values for  $\text{La}_{0.7}\text{Ca}_{0.3}\text{MnO}_3$  ( $T_c=233\text{ K}$ ),  $\text{La}_{2.1}\text{Ca}_{1.9}\text{Mn}_3\text{O}_{10}$  ( $T_c=184\text{ K}$ ), and  $\text{La}_{1.4}\text{Ca}_{1.6}\text{Mn}_2\text{O}_7$  ( $T_c=133\text{ K}$ ) are estimated to be 0.98, 0.77, and 0.56 eV, respectively. The reduction in  $W$  accompanied by a reduction in  $n$  was also demonstrated in the magnitudes of the electrical resistivities. The increase in electrical resistivity  $\rho$  with decreasing  $n$  (see Table I) is attributed to a narrowing of the one-electron bandwidth. This is expected from the basic concept of the double exchange model: both  $T_c$  and  $\rho$  reflect real charge motion determined by the transfer interaction  $t$ , via the one-electron bandwidth. It should be noted that the reduced  $W$  corresponds to that along the  $c$  axis rather than the  $a$  axis.

When discussing the  $n$  dependence of the MR effect, we first consider the effect of the bandwidth  $W$  of the  $e_g$  electron. The role of the bandwidth on the magnitude of MR have been suggested from the previous results on three-dimensional compounds with the different average ionic radius of the La site. It is shown that increasing the bond distortion enhances the MR response and reduces the ferromagnetic transition temperature  $T_c$ . Several reports on the three-dimensional compounds have shown a general trend that the MR response is nearly inversely proportional to the ferromagnetic transition temperature  $T_c$ . Within the framework of the recently developed Kondo lattice model,<sup>21</sup> the narrowing of the bandwidth results in both the lowering of the  $T_c$  and enhanced coupling ( $J_H/W$ ) between itinerant carriers and localized spins. To investigate the role of  $W$  in the relationship between the MR response and  $T_c$  and related issues in the present compounds, we plot in Fig. 4 the relationship between magnitude of the maximum MR (at 0.1 and 1 T) and the  $T_c^p$  values obtained in the present study ( $n=2,3$  and  $\infty$ ) and the previous studies ( $n=\infty$ ).<sup>2,3,6</sup> It is clear that the MR magnitude in the  $n=2$  compounds increases more rapidly with a decrease in  $T_c^p$ , and no (inverse) linear relationship can be seen between them. The deviation from the linear relationship is more evident in a low magnetic field (0.1 T). This indicates that we cannot attribute the enhanced MR of these two-dimensional compounds solely to the narrower bandwidth. An additional factor affecting the MR response is the spin correlation inherent to two-dimensional compounds. This is because spin-correlated fluctuation scattering has a dominant effect on the MR near  $T_c^p$ . To obtain an insight into these issues, we examined the field depen-

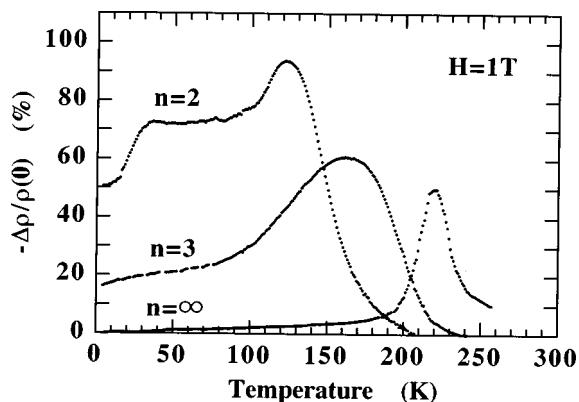


FIG. 3. Temperature dependence of MR ratio  $[-\Delta\rho/\rho(0)]$  for thin films of  $\text{La}_{n-nx}\text{Ca}_{1+nx}\text{Mn}_n\text{O}_{3n+1}$  with  $n=2, 3$ , and  $\infty$ . These data are measured under an applied magnetic field of 1 T.

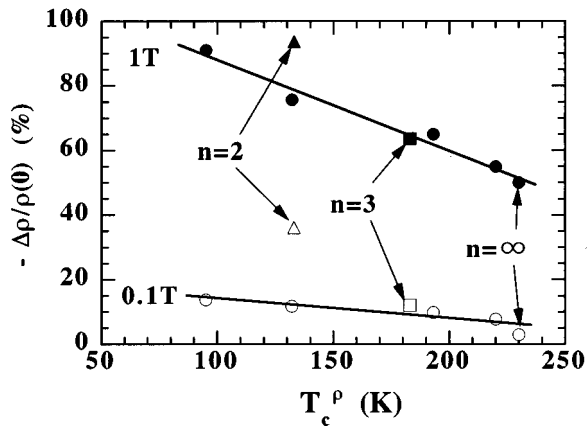


FIG. 4. MR ratio  $[-\Delta\rho/\rho(0)]$  in  $H=0.1$  T, and 1 T plotted against the  $T_c^p$  values for thin films of  $\text{La}_{n-nx}\text{Ca}_{1+nx}\text{Mn}_n\text{O}_{3n+1}$  in the present study ( $n=2, 3$ , and  $\infty$ ) and previous studies (Refs. 2, 3, and 6) ( $n=\infty$ ). The closed symbols denote data in  $H=1$  T, and the open symbols denote data in  $H=0.1$  T. The (open and closed) circles (indicated by arrows) denote present data for  $n=\infty$ , and the other circles denote reported data (Refs. 2, 3, and 6) for  $n=\infty$ . The squares denote data for  $n=3$ , and the triangles denote data for  $n=2$ .

dened of normalized resistivity  $\rho(H)/\rho(0)$  for the three thin-film samples at  $T_c^p$  and the results are shown in Fig. 5. In the  $\rho(H)/\rho(0)-H$  curves, a steep  $\rho(H)/\rho(0)$  decrease is observed in the low magnetic field range below 0.5 T, particularly for the  $n=2$  compound. The observed field dependence of the MR response shows that in the two-dimensional materials the spin-correlated fluctuation can be easily suppressed by a low external field. Recent studies suggest a two-dimensional and/or short-range spin correlation above  $T_c^p$  for the  $n=2$  compound.<sup>15,22</sup> Below  $T_c^p$ , the spin correlation becomes long range. The two-dimensional spin ordering in the layered compound possibly originates from the anisotropic exchange interactions in the  $a$ - $b$  axis (in-plane) and the  $c$ -axis (out-of-plane) directions. Larger anisotropy expected for a smaller  $n$  compound might lead to more enhanced two-dimensional fluctuation. The broad MR peak with an asymmetric shape seen in the MR- $T$  curve only for the  $n=2,3$  compounds (Fig. 3) may suggest that two-

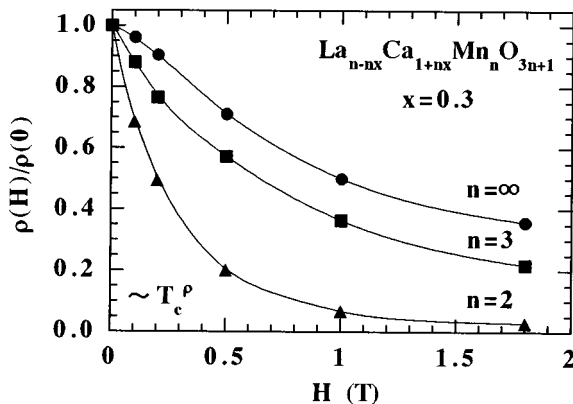


FIG. 5. Field dependence of normalized resistivity  $\rho(H)/\rho(0)$  at near  $T_c^p$  for the thin films of  $\text{La}_{n-nx}\text{Ca}_{1+nx}\text{Mn}_n\text{O}_{3n+1}$  with  $n=2, 3$ , and  $\infty$ . The solid lines are drawn only as a guide to the eyes.

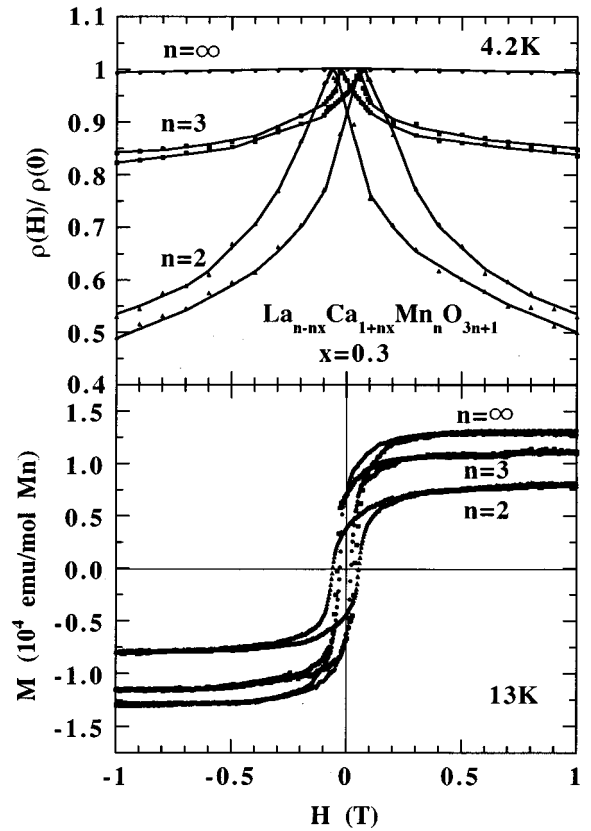


FIG. 6. Field dependence of normalized resistivity  $\rho(H)/\rho(0)$  and magnetization  $M$  at low temperatures for the thin films of  $\text{La}_{n-nx}\text{Ca}_{1+nx}\text{Mn}_n\text{O}_{3n+1}$  with  $n=2, 3$ , and  $\infty$ . The normalized resistivity  $\rho(H)/\rho(0)$  was measured at 4.2 K, and the magnetization  $M$  was measured at 13 K. These data were obtained after the initial application of a magnetic field of +1.8 T. The solid lines in the top panel are drawn only as a guide to the eyes.

dimensional spin-correlated fluctuations survive down to lower temperatures. The existence of two-dimensional spin-correlated fluctuations even in the ferromagnetic state may be associated with the observation of enhanced Jahn-Teller distortion upon charge delocalization for the double layer manganites.<sup>23</sup>

The most distinctive difference between the features of the three- and two-(layered) dimensional compounds is in their low-temperature MR behavior. The field dependence of normalized resistivity  $\rho(H)/\rho(0)$  and magnetization  $M$  for the three thin-film samples at low temperatures are shown in Fig. 6, and indicative of apparent hysteresis behavior for the  $n=2,3$  compounds. We found that the magnetic fields leading to the resistivity peak in the  $\rho(H)/\rho(0)-H$  curve correspond to the fields at which zero magnetization is obtained in the  $M-H$  curve. The observed MR with hysteresis behavior for the  $n=2,3$  compounds can be understood by the intragrain (intrinsic) spin-polarized tunneling through the insulating  $(\text{La,Ca})_2\text{O}_2$  layer. Moreover, it is found that the magnitude of the tunneling MR depends critically on the number (2 or 3) of  $\text{MnO}_2$  layers, as listed in Table I. This means that the magnitude of the tunneling MR is not solely determined by the spin polarization, since nearly complete spin polarization is also expected for the perovskite manganites at low temperatures. On the basis of the tunneling conductance network model,<sup>24</sup> we might explain such a large

difference by taking account of the additional magnetic energy in the tunneling process. When the magnetic moments of neighboring  $(\text{MnO}_2)_n$  layers separated by a  $(\text{La,Ca})_2\text{O}_2$  layer are not parallel and electron spin is conserved in the tunneling, additional magnetic exchange energy related to the  $c$ -axis transfer interaction is required. Further study is necessary to clarify the role of the transfer interaction and the spin configuration in the behavior of the tunneling MR.

In conclusion, we have reported results on the magnetotransport properties of  $\text{La}_{n-nx}\text{Ca}_{1+nx}\text{Mn}_n\text{O}_{3n+1}$  ( $n=2,3$ , and  $\infty$ ,  $x=0.3$ ) thin films. Our results demonstrate that a

reduction in the number of  $\text{MnO}_2$  layers in the unit cell resulted in systematic changes in various features. These changes include an increase in resistivity, a decrease in resistivity peak temperature  $T_c^p$  corresponding to the metal-insulator transition, an enhancement in the maximum MR near  $T_c^p$ , and an increase in the low-temperature intrinsic tunneling MR. A comparison of the magnitude of these features among these compounds suggested that both the reduced  $c$ -axis transfer interaction and the two-dimensional spin fluctuation play an important role in determining the CMR and related properties in layered manganites.

- 
- <sup>1</sup>R. von Helmolt, J. Wecker, B. Holzapfel, L. Schultz, and K. Samwer, *Phys. Rev. Lett.* **71**, 2331 (1993).  
<sup>2</sup>K. Chahara, T. Ohno, M. Kasai, and Y. Kozono, *Appl. Phys. Lett.* **63**, 1990 (1993).  
<sup>3</sup>M. McCormack, S. Jin, T. H. Tiefel, R. M. Fleming, J. M. Phillips, and R. Ramesh, *Appl. Phys. Lett.* **64**, 3045 (1994).  
<sup>4</sup>P. Schiffer, A. P. Ramirez, W. Bao, and S. W. Cheong, *Phys. Rev. Lett.* **75**, 3336 (1995).  
<sup>5</sup>H. Y. Hwang, S. W. Cheong, P. G. Radaelli, M. Marezio, and B. Batlogg, *Phys. Rev. Lett.* **75**, 914 (1996).  
<sup>6</sup>C. L. Canedy, K. B. Ibsen, G. Xiao, J. Z. Sun, A. Gupta, and W. J. Gallagher, *J. Appl. Phys.* **79**, 4546 (1996).  
<sup>7</sup>C. Zener, *Phys. Rev.* **82**, 403 (1951).  
<sup>8</sup>P. W. Anderson and H. Hasegawa, *Phys. Rev.* **100**, 675 (1955).  
<sup>9</sup>P. G. de Gennes, *Phys. Rev.* **118**, 141 (1960).  
<sup>10</sup>A. J. Millis, P. B. Littlewood, and B. I. Shraiman, *Phys. Rev. Lett.* **74**, 5144 (1995).  
<sup>11</sup>H. Roder, J. Zang, and A. R. Bishop, *Phys. Rev. Lett.* **76**, 1356 (1996).  
<sup>12</sup>A. Shengelaya, G. Zhao, H. Keller, and K. A. Muller, *Phys. Rev. Lett.* **76**, 5296 (1996).  
<sup>13</sup>Y. Moritomo, Y. Tomioka, A. Asamitsu, Y. Tokura, and Y. Matsui, *Nature (London)* **380**, 141 (1996).  
<sup>14</sup>H. Asano, J. Hayakawa, and M. Matsui, *Appl. Phys. Lett.* **68**, 3638 (1996).  
<sup>15</sup>H. Asano, J. Hayakawa, and M. Matsui, *Phys. Rev. B* **56**, 5395 (1997).  
<sup>16</sup>T. Kimura, Y. Tomioka, H. Kuwahara, A. Asamitsu, M. Tamura, and Y. Tokura, *Science* **274**, 1698 (1996).  
<sup>17</sup>D. N. Argyriou, J. F. Mitchell, J. B. Goodenough, O. Chamaissem, S. Short, and J. D. Joergensen, *Phys. Rev. Lett.* **78**, 1568 (1997).  
<sup>18</sup>H. Asano, J. Hayakawa, and M. Matsui, *Appl. Phys. Lett.* **71**, 844 (1997).  
<sup>19</sup>F. Fontcuberta, M. Martinez, A. Seffar, S. Pinol, J. L. Garcia-Munoz, and X. Obrador, *Phys. Rev. Lett.* **76**, 1122 (1996).  
<sup>20</sup>J. H. Park, C. T. Chen, S. W. Cheong, W. Bao, G. Meigs, V. Chakarian, and Y. U. Idzerda, *Phys. Rev. Lett.* **76**, 4215 (1996).  
<sup>21</sup>N. Furukawa, *J. Phys. Soc. Jpn.* **63**, 3214 (1994).  
<sup>22</sup>T. G. Perring, G. Aeppli, Y. Moritomo, and Y. Tokura, *Phys. Rev. Lett.* **78**, 3197 (1977).  
<sup>23</sup>J. F. Mitchell, D. N. Argyriou, J. D. Joergensen, D. G. Hinks, C. D. Potter, and S. D. Bader, *Phys. Rev. B* **55**, 63 (1997).  
<sup>24</sup>J. S. Helman and B. Abeles, *Phys. Rev. Lett.* **37**, 1429 (1976).